Mechanics Research Communications 42 (2012) 15–21

Contents lists available at SciVerse ScienceDirect

Mechanics Research Communications

journal homepage: www.elsevier.com/locate/mechrescom

Simulation of adaptation of blood vessel geometry to flow and pressure: Implications for arterio-venous impedance

Theo Arts*, Koen Reesink, Wilco Kroon, Tammo Delhaas

Department of Biomedical Engineering, Maastricht University, Maastricht, The Netherlands

ARTICLE INFO

Article history:
Received 1 September 2011
Received in revised form 7 October 2011
Available online 10 November 2011

Keywords:
Compliance
Pulse wave
Stress
Nonlinear
Remodeling

ABSTRACT

Aortic input impedance relates pressure to flow at the aortic entrance distal to the aortic valve. We designed the CircAdapt three-element model of this impedance, consisting of resistive wave impedance, arterial compliance and peripheral resistance. Direct association of the elements with physical properties facilitated incorporation of nonlinear elastic properties of wall material and adaptation of vessel geometry to mechanical load. Use of the CircAdapt impedance model is extended to all arterial and venous connections to the heart. After incorporation in the existing CircAdapt model of whole circulation dynamics, vascular geometry was determined by adaptation to hemodynamic load as generated by the CircAdapt model itself. Model generated vascular geometry and hemodynamics appear realistic. Since the same adaptation rules are used for arteries and veins, all vascular impedances are determined mainly by two parameters only. Thus, large changes in hemodynamic load, like exercise or hypertension, were simulated realistically without the need to change parameter values. Simulation of adaptation enables to predict consequences of chronic change in hemodynamics, e.g. due to pathology or proposed therapy.

1. Introduction

Pump load of the left ventricle is determined by the relation between pressure and flow in the outlet tract. Using similarity of hemodynamics with electrical circuitry, the pressure–flow relation is described quantitatively by the hemodynamic input impedance of the ascending aorta. This impedance is represented classically by the three-element Windkessel model (Westerhof et al., 1971, 2009), consisting of the resistive wave impedance R_{wave} in series with the parallel combination of an arterial compliance C_a and a peripherally located resistance R_2 (Fig. 1). The model can simulate realistically the diastolic aortic pressure decay and the effects of pulse wave propagation into the aorta.

In simulating patient hemodynamics, the model is assumed to be linear. Since arterial compliance and wave impedance are nonlinear, the validity range of the model is limited; unveiling an important shortcoming of the model that for each new hemodynamic state a new set of parameter values has to be estimated. Nonlinear behavior cannot be easily implemented because no accurate description of the relation between element parameters and physical properties of blood vessels is available (Westerhof et al., 2009).

Geometry of arteries adapts to mechanical load imposed by pressure and flow. In modeling an adaptation cycle, calculated deviations of mechanical load of the tissue in the walls from the standard values induce changes in arterial geometry. From the new geometry, the hemodynamic impedance should be derived, so that the new hemodynamic state can be simulated. By calculating the resulting mechanical load of the vessel wall, the control loop for regulation of vascular geometry is closed.

The primary goal of this study is to link parameter values of a model of the aortic input impedance to physical properties of the arterial system. The model should incorporate nonlinearity of the stress–strain relationship of vessel wall material, so that with change of hemodynamic state there is no need to re-estimate parameter values.

Besides the systemic arterial tree, other vascular trees have a similar structure, characterized by the possibility to propagate pulse waves and being connected to a peripheral microvasculature. Therefore, in the present study we have generalized the description of the aortic input impedance to the impedances of the pulmonary arterial system and the systemic and pulmonary veins. The resulting pressure–flow relations in the large arteries and veins have been incorporated in the CircAdapt model that describes hemodynamics of the whole circulation with a focus on the environment of the heart (Arts et al., 2005; Lumens et al., 2009).

Considering adaptation of geometry of blood vessels to hemodynamic load, wall thickness of arteries is known to increase with intra-arterial pressure (Arner et al., 1984). Additionally, the diameter of a blood vessel increases with increase of flow (Furchgott,

* Corresponding author at: Department of Biomedical Engineering, Maastricht University, PO Box 616, 6200MD Maastricht, The Netherlands. Tel.: +31 43 388 1659; mobile: +31 61 894 3830.
E-mail address: t.arts@maastrichtuniversity.nl (T. Arts).

0093-6413/$ – see front matter © 2011 Elsevier Ltd. All rights reserved.
doi:10.1016/j.mechrescom.2011.10.005

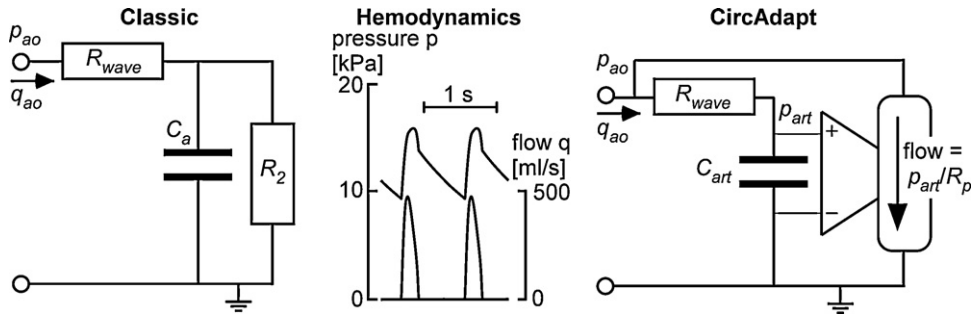

Fig. 1. Left: Classic three-element Windkessel model of aortic input impedance (Westerhof et al., 1971) with tracings of pressure and flow (mid). Right: Modification to the CircAdapt impedance, where the elements are more closely linked to physical properties of the arterial system. Symbols R_{wave}, R_2 and C_a indicate wave impedance, peripheral resistance component and compliance of the classic representation. Symbols R_p and C_{art} indicate true peripheral resistance and arterial compliance, directly inserted in the CircAdapt impedance.

1983; Reneman et al., 2006). The latter two adaptation mechanisms have been simulated and incorporated in the CircAdapt model. For all arteries and veins, the same universal adaptation rules have been applied. As a result, geometry of all large blood vessels is determined by a relatively small set of parameters, related to general properties of vascular tissue.

2. Model description

2.1. CircAdapt modification of three-element arterial input impedance

The classic three-element Windkessel model of arterial input impedance approximates the true impedance quite well, but the constituting elements have no direct relation with physical properties of the arterial system. Peripheral resistance R_p, defined as the ratio of mean aortic pressure over mean aortic flow is the sum of wave impedance R_{wave} and resistance R_2 in Fig. 1. Arterial compliance C_{art} represents the compliance of the whole arterial volume proximal to the peripheral resistance located in the arterioles. Compliance C_a in Fig. 1 is chosen so that time constant R_2C_a equals R_pC_{art}. Thus it holds

$$R_2 = R_p - R_{wave}, \quad C_a = \frac{R_pC_{art}}{R_p - R_{wave}} \tag{1}$$

It follows that compliance C_a is an overestimation of true arterial compliance C_{art} (Segers et al., 1999). Conversely, mean pressure over the compliance C_a is lower than mean aortic pressure, implying that pressure over C_a is an underestimate of the true mean arterial pressure.

To simplify relationships between physical properties and model parameters, we designed a new three-element arterial input impedance, shown in Fig. 1 as the CircAdapt representation. In this representation, the three constituting elements R_{wave}, R_p, and C_{art} are linked directly to physical properties of the arterial system. The major modification is the implementation of the peripheral resistance as a flow source, connected to the aortic entrance, and which flow equals the pressure difference over the arterial compliance, divided by peripheral resistance R_p. When assuming linearity of the constituting elements, the classic and CircAdapt representations behave identically, applying the conversion presented in Eq. (1).

In relating the properties of the elements to the mechanical properties of the vessel wall, first we describe the stress–strain relation of vessel wall material. Incorporation of these properties in the geometry of the vessel wall renders the pressure–area relation. From this relation, the characteristic wave impedance and arterial compliance are calculated.

2.2. Nonlinear pressure–area relation

Blood vessel wall material is assumed to be composed of force bearing nonlinearly elastic fibers, like elastin and collagen, embedded in incompressible soft material. Wall material of blood vessels is nonlinearly elastic, behaving stiffer at larger extensions. We used an exponential relation between fiber stress σ_f and natural fiber strain ε_f:

$$\sigma_f = \sigma_{f,ref}\exp(k\varepsilon_f) \quad \text{with natural strain definition,} \quad \varepsilon_f = \ln\left(\frac{L}{L_{ref}}\right) \tag{2}$$

Parameter k characterizes fiber stiffness. Symbols L and L_{ref} represent length of a fiber segment and its reference value, respectively. Parameter $\sigma_{f,ref}$ is a material constant. Assuming the wall to be thin, mean fiber stress σ_f and strain $\Delta\varepsilon_f$, are related to internal pressure p and the ratio of cavity to wall volume V_c/V_w by a first order approximation of the previously published higher order approximation (Arts et al., 1991)

$$\frac{p}{\sigma_f} = \frac{1/3}{V_c/V_w + (1/2)} \tag{3}$$

$$\Delta\varepsilon_f = \Delta\int \frac{p}{\sigma_f} d\left(\frac{V_c}{V_w}\right) = \frac{1}{3}\Delta\ln\left(\frac{V_c}{V_w} + \frac{1}{2}\right) \tag{4}$$

For strain a reference state is defined, where pressure p and volume V_c equal their reference values p_{ref} and $V_{c,ref}$, respectively. Strain $\Delta\varepsilon_f$ as calculated with Eq. (4) is substituted in Eq. (2), rendering an expression for fiber stress σ_f. By substitution of the result in Eq. (3) and using that pressure p equals reference pressure p_{ref} at reference volume $V_{c,ref}$, it follows:

$$p = p_{ref}\left(\frac{V_c/V_w + (1/2)}{V_{c,ref}/V_w + (1/2)}\right)^{k/3-1} \tag{5}$$

Whereas for better practical understanding, two parameters p_{ref} and $V_{c,ref}$ are used. Both parameters actually form together a single constant, thus representing only one independent parameter. Assuming that the volume ratio V_c/V_w equals the ratio of the corresponding ratio of cross-sectional areas A_c/A_w, it is found:

$$p = p_{ref}\left(\frac{A_c/A_w + (1/2)}{A_{c,ref}/A_w + (1/2)}\right)^{k/3-1} \tag{6}$$

2.3. Wave impedance and arterial compliance impedance

Arterial input impedance is characterized by elements peripheral resistance R_p, characteristic wave impedance R_{wave} and arterial

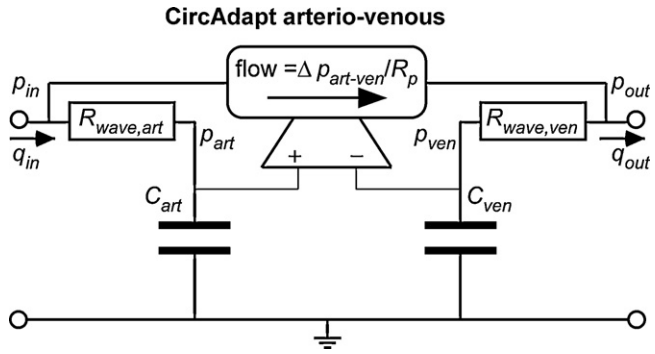

Fig. 2. CircAdapt model of arterio-venous hemodynamic impedance. Symbols *p*, *q*, *R* and *C* indicate pressure, flow, resistance and compliance, respectively. Subscripts *art*, *ven*, *wave*, and *p* indicate arterial, venous, wave and peripheral, respectively.

compliance C_{art}. Resistance R_p equals the ratio of mean aortic pressure over mean aortic flow. In the CircAdapt impedance model, volume V_c of the arterial compliance is a state variable of the related differential equation. Arterial pressure p_{art} is calculated from this volume as pressure p in Eq. (5). Impedance R_{wave} and compliance C_{art} are written as a function of p_{art}.

For a cylindrical blood vessel, R_{wave} depends on inertia and compliance of the blood vessel by the general equation, presented as the middle term in Eq. (7) (Bramwell and Hill, 1922). Application of the general equation to Eq. (6) renders wave impedance as a function of p_{art}:

$$R_{wave} = \sqrt{\frac{\rho}{A_c}\frac{dp_{art}}{dA_c}} = \sqrt{\frac{\rho(k/3-1)p_{art}}{A_c(A_c+(1/2)A_w)}} \tag{7}$$

Symbol ρ indicates blood density. Previously, a characteristic length was defined so that volume of the arterial system was equal to the product of this length and the proximal arterial cross-section (Wesseling et al., 1993). Likewise, we defined the characteristic length L_c of the arterial system so that arterial compliance C_{art} equals the product of this length and cross-sectional compliance at the arterial entrance:

$$C_{art} = L_c\frac{dA_c}{dp_{art}} = \frac{L_c(A_c+(1/2)A_w)}{(k/3-1)p_{art}} \tag{8}$$

In many studies, arterial stiffness is quantified by pulse wave velocity. In our model, parameter k is a main determinant of vessel wall stiffness. Wave velocity v_{wave} depends on inertia and compliance of the blood vessel by the general equation presented as the middle term of Eq. (9) (Bramwell and Hill, 1922). Application of this equation to Eq. (6) renders v_{wave} as a function of pressure p_{art} and stiffness parameter k:

$$v_{wave} = \sqrt{\frac{A_c}{\rho}\frac{dp_{art}}{dA_c}} = \sqrt{\frac{(k/3-1)\,p_{art}}{\rho(1+(1/2)A_w/A_c)}} \tag{9}$$

2.4. Coupling of arterial to venous impedance

As seen from the heart, pulse waves propagate into the aorta, resulting in the CircAdapt description of aortic input impedance (Fig. 1). As seen from the right atrium, waves propagate backward into veins, resulting in a similarly structured impedance at the venous side. Furthermore, the ratio of mean arterio-venous pressure difference to mean flow equals systemic peripheral resistance R_p. So, for the simulation of the systemic vasculature, the aortic impedance is extended to the symmetrically structured CircAdapt arterio-venous (AV-) impedance, where the peripheral resistance is simulated by a flow source, controlled by the pressure difference between the arterial and venous compliances (Fig. 2). Arterial and venous wave impedances and compliances are calculated with Eqs. (7) and (8). In the CircAdapt model of the whole circulation, the proposed arterio-venous impedance has been applied for systemic as well as pulmonary circulations. Although not carried out yet, the same AV-impedance design may be used to represent any peripheral subsystem of the circulation, e.g. that of an organ.

2.5. Adaptation of vessel geometry to pressure and flow

In the CircAdapt model, wall thickness of a blood vessel adapts to internal pressure so that maximal wall stress is kept at a fixed level $\sigma_{f,\max}$. Since blood vessels must withstand extremes, wall thickness is simulated to adapt to the highest level of wall stress occurring, i.e. that during maximum exercise. So, for growth of wall thickness we used:

$$\frac{\tau_{Aw}}{A_w}\frac{dA_w}{dt} = \frac{\sigma_f}{\sigma_{f,\max}} - 1 \tag{10}$$

Parameter τ_{Aw} represents the time constant of adaptation, which is assumed to be in the order of days or weeks. Note that for arteries, highest levels of fiber stress σ_f occur in systole when pressure is maximal. For veins, the pressure pulse as induced by the heart is small. However, especially during exercise, the body is subject to accelerations due to motion, causing flow shock waves in all blood vessels. Pressure amplitude p_{impact} of a shock wave depends on body impact velocity v_{impact} by Arts et al. (2005)

$$p_{impact} = A_c v_{impact} R_{wave} = \rho v_{impact} v_{wave} \tag{11}$$

The third term of Eq. (11) maybe more convenient to use and is derived with Eq. (7,9). Adding of hemodynamic and impact pressure components renders total pressure load of the blood vessel to which wall thickness is simulated to adapt.

Vessel diameter is strongly indicated to be controlled by the time average of shear stress along the inner wall (Brownlee and Langille, 1991; Dammers et al., 2002; Kelly and Snow, 2007) in resting condition. Assuming a parabolic mean flow profile, mean shear stress σ_s depends on vessel diameter D, flow q and blood viscosity η by:

$$\sigma_s = \frac{32\eta q}{\pi D^3} \tag{12}$$

Small vessels appear to regulate mean shear stress to a fixed level $\sigma_{s,ref}$. However, in larger blood vessels the level of shear stress appears to be lower (Dammers et al., 2002; Tangelder et al., 1988). The latter observation has been implemented by the following modification of the original CircAdapt model for diameter adaptation:

$$\frac{\tau_D}{D}\frac{dD}{dt} = 1 - \frac{\pi D^3\gamma_{s,ref}}{32q(1+D/h)} \quad \text{with} \quad \gamma_{s,ref} = \frac{\sigma_{s,ref}}{\eta} \tag{13}$$

Parameter τ_D represents the time constant of diameter adaptation. For convenience, a single parameter $\gamma_{s,ref}$ is used instead of the pair of parameters $\sigma_{s,ref}$ and η. Parameter h indicates the diameter, above which vessel dilation is more sensitive to shear stress.

2.6. Implementation

The proposed CircAdapt arterio-venous impedance, together with the adaptation rules, is implemented in the modular CircAdapt model to simulate beat-to-beat hemodynamics of circulation as a whole, including the heart (Fig. 3) (Arts et al., 2005; Lumens et al., 2009). Atria and ventricles are simulated by contractile chambers. Both ventricles are mechanically coupled. Simulations render time courses of pressures and flows in heart and blood vessels. The CircAdapt model offers the possibility to adapt geometry of its components to their mechanical and hemodynamic load, as computed by the model itself. Characteristic parameter values related to the

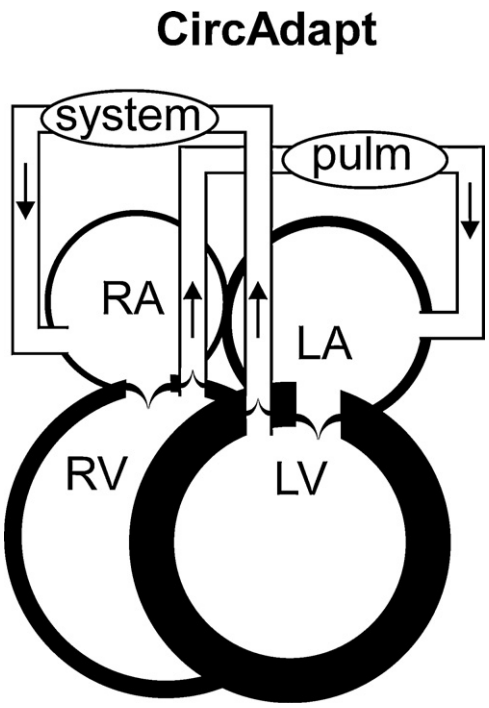

Fig. 3. The CircAdapt model of whole circulation dynamics. Left (LA) and right (RA) atria are cavities with a muscular wall. Left (LV) and right (RV) ventricle are cavities, formed by three mechanically coupled walls. Systemic (system) and pulmonary (pulm) circulations consist of trees of elastic tubes, connected by their microvasculature. The model generates pressures and volumes of all cavities and flows through all valves and blood vessels as a function of time during the cardiac cycle.

large blood vessels are listed in Table 1. Note that no distinction is made between arteries and veins. Stiffness constant k and both characteristic lengths L_c have been chosen so that the time courses of aortic and pulmonary pressure are typical. Parameter $\gamma_{s,ref}$ has been determined experimentally in arterioles (Tangelder et al., 1988). Parameters $\sigma_{f,max}$ and h have been chosen so that adapted aortic geometry is physiological. Body impact velocity v_{impact} is based on a jump of the body from a height of 0.5 meter. Time constants of adaptation τ_{Aw} and τ_D are not mentioned, since they do not influence the final state of adaptation.

2.7. Simulations

With the CircAdapt model of the whole circulation, simulations were carried out at rest and with exercise. In the resting state mean aortic blood flow was 85 ml/s (≈5.6 l/min), mean arterial pressure was 12.2 kPa (92 mmHg) and heart rate was 72 beats/min. In the state of exercise, aortic flow was multiplied by 3.0, and heart rate was doubled. Vessel geometry was adapted so that maximum wall stress with exercise and shear rate at rest reached the level of adaptation (Table 1). Next, hypertension was simulated by multiplication of mean aortic blood pressure with a factor of 1.5. The protocol of adaptation to hypertension was carried out to show changes in vascular geometry.

Table 1
Parameters relevant for blood vessel hemodynamics and adaptation.

Parameter	Value	Unit	Meaning
ρ	1050	kg/m^3	Density of blood (Eq. (7))
v_{impact}	3.0	m/s	Impact velocity (Eq. (11))
L_c	0.70	m	Characteristic length systemic blood vessel (Eq. (8))
	0.20	m	Characteristic length pulmonary blood vessel
k	12	–	Stiffness constant (Eq. (3))
$\sigma_{f,max}$	500	kPa	Maximum wall stress (Eq. (10))
$\gamma_{s,ref}$	1700	1/s	Reference of small vessel shear rate (Eq. (13))
h	0.9	mm	Vessel diameter transition for adaptation (Eq. (13))

3. Results

In Fig. 4 time courses of pressures and flows are shown for the large blood vessels and cardiac cavities under resting conditions after adaptation. Left and right ventricular cavities are separated from the arteries by valves, causing diastolic cavity pressure and arterial pressure to separate. Pulsations in flow and pressure are about in phase, indicating that arterial flow waves propagate downstream. The ratio of pulse pressure to mean pressure is significantly higher in the pulmonary arteries than in the aorta. At the connection sites of the veins to the atria, pressure and flow changes are clearly in anti-phase, indicating that venous flow waves propagate upstream. Since there are no valves, venous and atrial pressures are close. Existing pressure differences are due to hemodynamic acceleration effects.

Geometry of blood vessels forms automatically by adaptation. Variations in initial dimensions before adaptation by ±50% resulted in the same final solution, indicating that the found solution for geometry is unique in the physiological range. Data on obtained geometry is shown in Table 2. As expected, blood vessels carrying high pressure load have a thicker wall. For arteries, maximum pressure load during exercise, having the effect of body impact velocity included, is about a factor 2 of that pressure load during systole at rest. For veins this factor is much larger, up to a factor of 16. At a closer look, this difference is attributed to a relatively fixed pressure contribution of impact velocity, while in veins regular hemodynamic pressure load becomes practically negligible for adaptation of wall thickness.

As expected, with hypertension, aortic wall thickness increases most (Table 2). Wall thickness of the pulmonary veins increases also because of increasing left ventricular diastolic pressure (Fig. 4, right). Increase of pulmonary venous pressure elevates pulmonary arterial pressure, also to be noted by a diastolic wave in the pressure tracing. Since pressure increases also in the right-sided vessels, their walls also thicken to some extent. Note that diameters of large vessels (Table 2) are based on the assumption that all parallel vessel connections to the heart are combined to a single representative conduit. The real situation is quite different. For instance, the pulmonary trunk is short, readily splitting in two branches. Systemic venous return occurs by inferior and superior veins, entering the short chamber like caval vein, which directly connects to the right atrium. Four pulmonary veins enter the left atrium independently.

4. Discussion

In this study a novel hemodynamic input impedance of the arterial system is presented as an alternative of the classic three-element Windkessel model (Westerhof et al., 1971). The new CircAdapt impedance model consists of a wave impedance, arterial compliance and peripheral resistance. The advantage of this representation over the classic one is that each element is closely linked to specific physical properties of the arterial system. Wave impedance depends on diameter and elastic properties of the proximal aorta. Arterial compliance is determined by volume and elastic properties of the arterial system. Volume of the arterial system is an anatomical variable, closely linked to the product of proximal aortic cross-sectional compliance and a representative length of the arterial system, which depends mainly on anatomical size of the subject to be estimated by direct observation.

In the classic Windkessel representation, element parameters have to be derived from abovementioned impedance elements by conversion equations (Eq. (1)). Peripheral resistance, being the ratio

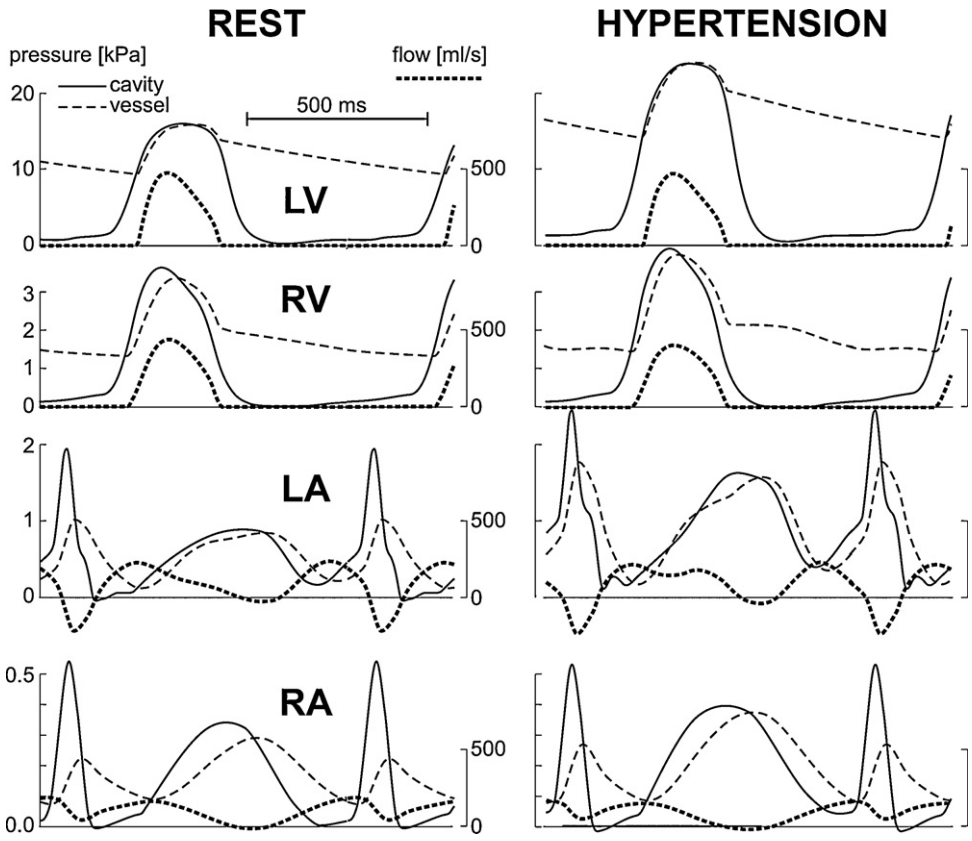

Fig. 4. CircAdapt simulation of pressures and flows at the connection sites of the large arteries and veins to the corresponding cardiac cavities LV, RV, LA and RA, respectively, at rest (left) and with systemic hypertension (right). Pressures in the cavities are also depicted. Note that in arteries pressures and flows are in phase, indicating forward waves. In veins pressures and flows are in anti-phase, indicating backward waves. Note differences in pressure scaling (1 kPa = 7.5 mmHg).

of mean aortic pressure and flow, varies with the level of exercise. When peripheral resistance approaches wave impedance, conversion to the classic Windkessel model is even not possible because of zero division in Eq. (1). With the CircAdapt impedance no difficulty is encountered. This finding is consistent with the problematic estimation of Windkessel parameters for the pulmonary circulation at low peripheral resistance (Segers et al., 1999). In the latter study it was also found that the arterial compliance as estimated with the classic model was significantly higher than this compliance as determined with the pulse contour method. The latter observation confirms our theoretical result that in the classic model the compliance is always larger than the true arterial compliance (Eq. (1)), and that this overestimation increases if peripheral resistance approaches wave impedance.

When assuming linear behavior of the elements, the classic and CircAdapt representation behave identically after proper conversion of values for compliance and resistances (Eq. (1)). If some physical phenomena behave nonlinearly, in the CircAdapt impedance model, these nonlinearities remain linked to the constituting elements by known relations. In the classic description, effects of these nonlinearities spread out further over different elements, thus complicating description and interpretation of nonlinear behavior. The nonlinear vessel stress–strain relationship of the vessel wall affects both wave impedance and arterial compliance (Eqs. (7) and (8)). Using this knowledge, nonlinear elastic behavior was incorporated in the CircAdapt impedance model, thus increasing the validity range for hemodynamic changes without the need to re-estimate parameters.

The latter increase in validity range is indicated by the following finding. Using the conventional linear three element model of aortic impedance, we estimated peripheral resistance, wave impedance and arterial compliance from the pressure and flow tracings in the

Table 2
Vessel geometry after simulated adaptation.

Vessel type	Lumen area (cm^2)	Wall area (cm^2)	Mean[a] pressure (kPa)	Systolic[a] pressure (mm)	Max[b] pressure (mm)	Internal diameter	Wall thickness
Rest							
Aorta	4.99	1.17	12.2	16.8	31.8	25.2	2.79
Pulmonary artery	4.97	0.46	1.96	3.69	10.9	25.2	1.13
Pulmonary vein	5.20	0.40	0.61	1.25	8.3	25.7	0.96
Systemic vein	5.14	0.28	0.18	0.32	4.9	25.6	0.68
Hypertension							
Aorta	4.98	2.01	18.3	24.1	48.4	25.2	4.65
Pulmonary artery	4.97	0.60	2.26	4.03	14.9	25.2	1.47
Pulmonary vein	4.98	0.65	0.94	1.78	11.9	25.2	1.59
Systemic vein	4.99	0.24	0.21	0.38	6.3	25.2	0.84

[a] Mean and systolic pressure at rest.
[b] Maximum pressure during exercise with the effect of impact included.

normal state and with hypertension, as presented in Fig. 4. The hypertension to normal ratio of estimated peripheral resistance, wave impedance and arterial compliance appeared to be 1.49, 1.56, and 0.71, respectively. These multiplication factors are so large that in analyzing hypertension, these parameters must be re-estimated, whereas with our new approach no parameters had to be changed.

The need to consider nonlinearity of the aortic input impedance has been questioned by Fogliardi et al. (1996). In that study arterial compliance was taken to be an exponential function of pressure, while wave impedance was a constant, not depending on vessel wall elasticity. In our model, arterial compliance is differently related to pressure, i.e. by a reciprocal relationship (Eq. (8)). Furthermore, wave impedance is related to compliance by using their common dependency on vessel wall elasticity. So, our nonlinearity is physically more consistent, and the number of independent parameters is reduced. Consequently, all parameters could be identified unambiguously. In the study by Fogliardi et al. it was concluded that identification of their nonlinearity parameters is troublesome. Apparently, modeling by physical understanding is a key to realistic implementation of nonlinearity.

Instead of applying conventional constitutive relationships, e.g. by using Young's modulus, well suited to simulate rubber like elastic properties, we postulated that deformation energy is stored in a nonlinearly elastic matrix of fibers embedded in soft, incompressible material (Arts et al., 1991). By assuming an exponential stress–strain relation (Eq. (2)) of these fibers, a power law relation is found for the pressure-area relation (Eq. (6)) with parameter k being a main determinant of vessel wall stiffness. In the human common carotid artery, pressure has been reported to depend exponentially on cross-sectional area ($p/p_{ref} = \exp(\alpha A/A_{ref})$ (Meinders and Hoeks, 2004)). In that study the exponent α for age intervals 20–30–40–50–60–70–80 years, was found to be 1.9, 2.3, 3.3, 3.6, 4.5 and 4.2, respectively. Using Eq. (6), it holds $k/3 - 1 \approx \alpha$. Thus, corresponding k-values are 8.7, 9.9, 12.9, 13.8, 16.5 and 15.6, respectively. According to Eq. (9), wave velocity is proportional with the square root of pressure. In canine coronary arteries (Arts et al., 1979), this velocity appeared proportional with pressure to the power 0.69. The corresponding k-value was calculated to be 23. In the common carotid artery of 25- and 75-year-old humans (Hermeling et al., 2010), wave velocity was 4.3 and 7.4 m/s, respectively, corresponding to k-values of 7.5 and 16.3. These data confirm that stiffness of arteries increases with age and decreases with vessel diameter.

An interesting effect of nonlinearity concerns decay of aortic pressure after closure of the aortic valve. Classically, the decay would be exponential. Taking into account the increase of arterial compliance with decreasing pressure, pressure decay is theoretically derived to be proportional with $1/(1 + t/\tau_{RC})$ with t and τ_{RC} representing time and a fixed time constant. Our solution and the exponential solution are similar shortly after aortic valve closure. Late after aortic valve closure, however, occurring for instance after cardiac arrest, the CircAdapt solution for pressure decay is considerably slower than exponentially. This finding is confirmed in patients with temporary cardiac arrest (Kottenberg-Assenmacher et al., 2009). Although in the latter study, the slow decay is presumed to be exponential, converging assymptotically to a positive pressure level, the experimentally measured pressure curve agrees much better with the above-mentioned $1/(1 + t/\tau_{RC})$ solution.

Previously, for the left ventricle the ratio of pressure to fiber stress (Eq. (3)) has been derived to be $1/3\ \ln(1 + V_w/V_c)$ (Arts et al., 1991). Here we have used the simpler, first order approach, mainly because vessel walls are relatively thin as compared to the wall of the left ventricle. For the thickest wall, i.e. that of the aorta, the relative error of the current approximation of pressure is less than 1.5%. To satisfy the condition that generated mechanical work by stress and strain in the wall equals the hemodynamic work of pressure and volume change, the corresponding equation for strain became much simpler, as presented in Eq. (4). Furthermore, Eqs. (5)–(9) became much simpler too.

The application of the CircAdapt impedance model has been extended to arterial and venous blood vessel trees in general. Arterial and venous impedances are coupled back to back by a peripheral resistance in between. Thus, 10 parameters are needed to describe hemodynamic behavior of the systemic and pulmonary circulation as seen from the heart. By attributing adaptation properties to blood vessel wall material in general, the number of parameters is reduced to 7 (Table 1). Since the diameter of all large vessels is much larger than parameter h, parameters h and $\gamma_{s,ref}$ can be combined to a single parameter $h\gamma_{s,ref}$ (Eq. (13)). Characteristic length L_c of systemic and pulmonary system is determined by body size, and may be set on forehand. When assuming a thin wall ($A_w \ll A_c$), using Eqs. (7)–(9), wall thickness appears of little influence on vessel compliance. The latter paradoxical finding is explained by the exponential behavior of the stress–strain relation (Eq. (2)). Since stiffness is the derivative of stress versus strain, stiffness is proportional with stress. With a thicker wall, stress decreases, causing stiffness to decrease, just so that total wall stiffness is maintained due to the thicker wall. Because wall thickness is less relevant, the importance of parameters $\sigma_{f,max}$ and v_{impact} is reduced. Summarizing, the hemodynamic properties of all large blood vessels together are determined mainly by only two parameters, i.e. stiffness constant k and a shear rate level, determined by the product $h\gamma_{s,ref}$.

Shear stress cannot be the only factor determining vessel diameter regulation. Shear rate is inversely proportional with the third power of vessel radius (Eq. (12)). When regulating diameter so that shear rate is constant, mean flow is expected to be proportional to the third power of diameter. Then, for a symmetric bifurcation the ratio of summed area of two distal branches to the area of the proximal branch would be 1.26. For porcine coronary arteries it is found that this ratio decreases with increasing artery diameter, from 1.3 for small (10 μm) diameters to about 1.0 for large (3 mm) diameters (VanBavel and Spaan, 1992). These findings imply that for small vessels mean flow is proportional with the third power of the diameter, and for large vessels proportional with the square of the diameter. In a study on canine coronary arteries (Arts et al., 1979) in the diameter range 0.5–3.0 mm, mean flow is found to be proportional with diameter to the power 2.55, which is intermediate between 2 and 3. This finding is much in agreement with the aforementioned study. Remarkably, in mammals, mean aortic flow velocity appears to be independent of size of animal and aorta (Dawson, 2001), indicating that flow in the aorta is proportional to the square of the diameter. These findings suggest that the level of mean shear rate and shear stress diminishes with increasing artery diameter. Apparently, in the largest arteries shear rate diminishes reciprocally with the diameter, and in the small ones shear rate is about constant. Therefore, we assumed a critical diameter h (Table 1, Eq. (12)), below which sensitivity to shear stress is constant, and above which this sensitivity increases linearly with diameter. In rabbit arterioles, shear rate is found to be 1700 s^{-1} with a large range (470–4700 s^{-1}) around. In canine coronary arteries with diameters in the range of 0.5–3.0 mm (Arts et al., 1979), flow appeared proportional with diameter to the power 2.55, indicating that the diameter range is around the transition diameter h. In our simulation we obtained a best fit for humans by using a h-value of 0.9 mm (Table 1).

5. Conclusions

The classic three-element Windkessel model of aortic input impedance is a wave impedance in series with the parallel

combination of a compliance and a second resistance. We modified the impedance to the CircAdapt version in order to (1) facilitate association of element parameters to physical properties of arteries, (2) extend application to pulmonary arteries and large veins, (3) simulate the effect nonlinear elastic properties of the vessel wall, and (4) simulate adaptation of vessel wall geometry to hemodynamic load.

By application of the same adaptation characteristics to all arteries and veins, impedances of these blood vessels are mainly determined by only two parameters, one for vessel wall stiffness and one for shear rate. Vessel wall thickness appeared of little importance for elastic behavior, but is important for withstanding pressure load. Regulation of wall thickness requires a third parameter.

The validity range of the CircAdapt impedance is extended to nonlinear elastic behavior of vessel wall mechanics and to situations where wave impedance approaches peripheral resistance, such as in the pulmonary arterial system and with exercise.

Implementation of the novel three-element impedance in the existing CircAdapt model of circulation hemodynamics enables (1) simulation of large changes in hemodynamics, e.g. exercise, without change of parameter values, and (2) simulation of adaptation to a chronic change of hemodynamics, e.g. related to pathology or proposed therapies.

References

Arner, A., Malmqvist, U., Uvelius, B., 1984. Structural and mechanical adaptations in rat aorta in response to sustained changes in arterial pressure. Acta Physiol. Scand. 122, 119–126.

Arts, T., Bovendeerd, P.H.M., Prinzen, F.W., Reneman, R.S., 1991. Relation between left ventricular cavity pressure and volume and systolic fiber stress and strain in the wall. Biophys. J. 59, 93–103.

Arts, T., Delhaas, T., Bovendeerd, P., Verbeek, X., Prinzen, F.W., 2005. Adaptation to mechanical load determines shape and properties of heart and circulation, the CircAdapt model. Am. J. Physiol. 288, 1943–1954.

Arts, T., Kruger, R.T.I., Van Gerven, W., Lambregts, J.A.C., Reneman, R.S., 1979. Propagation velocity and reflection of pressure waves in the canine coronary artery. Am. J. Physiol. 237, H469–H474.

Bramwell, J., Hill, A., 1922. The velocity of the pulse wave in man. Proc. R. Soc. Lond. Ser. B 93, 298–306.

Brownlee, R.D., Langille, B.L., 1991. Arterial adaptations to altered blood flow. Can. J. Physiol. Pharmacol. 69, 978–983.

Dammers, R., Tordoir, J.H., Welten, R.J., Kitslaar, P.J., Hoeks, A.P., 2002. The effect of chronic flow changes on brachial artery diameter and shear stress in arteriovenous fistulas for hemodialysis. Int. J. Artif. Organs 25, 124–128.

Dawson, T.H., 2001. Similitude in the cardiovascular system of mammals. J. Exp. Biol. 204, 395–407.

Fogliardi, R., Di Donfrancesco, M., Burattini, R., 1996. Comparison of linear and nonlinear formulations of the three-element Windkessel model. Am. J. Physiol. 271, H2661–H2668.

Furchgott, R.F., 1983. Role of endothelium in responses of vascular smooth muscle. Circ. Res. 53, 557–573.

Hermeling, E., Hoeks, A.P., Winkens, M.H., Waltenberger, J.L., Reneman, R.S., Kroon, A.A., Reesink, K.D., 2010. Noninvasive assessment of arterial stiffness should discriminate between systolic and diastolic pressure ranges. Hypertension 55, 124–130.

Kelly, R.F., Snow, H.M., 2007. Characteristics of the response of the iliac artery to wall shear stress in the anaesthetized pig. J. Physiol. 582, 731–743.

Kottenberg-Assenmacher, E., Aleksic, I., Eckholt, M., Lehmann, N., Peters, J., 2009. Critical closing pressure as the arterial downstream pressure with the heart beating and during circulatory arrest. Anesthesiology 110, 370–379.

Lumens, J., Delhaas, T., Kirn, B., Arts, T., 2009. Three-Wall Segment (TriSeg) model describing mechanics and hemodynamics of ventricular interaction. Ann. Biomed. Eng.

Meinders, J.M., Hoeks, A.P., 2004. Simultaneous assessment of diameter and pressure waveforms in the carotid artery. Ultrasound Med. Biol. 30, 147–154.

Reneman, R.S., Arts, T., Hoeks, A.P., 2006. Wall shear stress—an important determinant of endothelial cell function and structure—in the arterial system in vivo. Discrepancies with theory. J. Vasc. Res. 43, 251–269.

Segers, P., Brimioulle, S., Stergiopulos, N., Westerhof, N., Naeije, R., Maggiorini, M., Verdonck, P., 1999. Pulmonary arterial compliance in dogs and pigs: the three-element Windkessel model revisited. Am. J. Physiol. 277, H725–H731.

Tangelder, G.J., Slaaf, D.W., Arts, T., Reneman, R.S., 1988. Wall shear rate in arterioles in vivo: least estimates obtained from platelet velocity profiles. Am. J. Physiol. 254, H1059–H1064.

VanBavel, E., Spaan, J.A., 1992. Branching patterns in the porcine coronary arterial tree. Estimation of flow heterogeneity. Circ. Res. 71, 1200–1212.

Wesseling, K.H., Jansen, J.R., Settels, J.J., Schreuder, J.J., 1993. Computation of aortic flow from pressure in humans using a nonlinear, three-element model. J. Appl. Physiol. 74, 2566–2573.

Westerhof, N., Elzinga, G., Sipkema, P., 1971. An artificial arterial system for pumping hearts. J. Appl. Physiol. 31, 776–781.

Westerhof, N., Lankhaar, J.W., Westerhof, B.E., 2009. The arterial Windkessel. Med. Biol. Eng. Comput. 47, 131–141.